Article

Self-Assembly, Structure, and Dynamic Interconversion of Metallosupramolecular Architectures Generated by Pb(II) Binding-Induced Unfolding of a Helical Ligand

Mihail Barboiu, Gavin Vaughan, Roland Graff, and Jean-Marie Lehn

J. Am. Chem. Soc., **2003**, 125 (34), 10257-10265• DOI: 10.1021/ja0301929 • Publication Date (Web): 01 August 2003

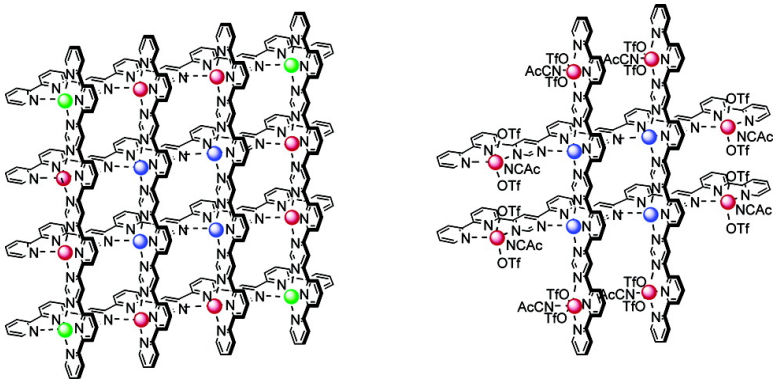

More About This Article

Additional resources and features associated with this article are available within the HTML version:

- Supporting Information
- Links to the 8 articles that cite this article, as of the time of this article download
- Access to high resolution figures
- Links to articles and content related to this article
- Copyright permission to reproduce figures and/or text from this article

View the Full Text HTML

J|A|C|S
ARTICLES
Published on Web 08/01/2003

Self-Assembly, Structure, and Dynamic Interconversion of Metallosupramolecular Architectures Generated by Pb(II) Binding-Induced Unfolding of a Helical Ligand

Mihail Barboiu,[†,‡] Gavin Vaughan,[§] Roland Graff,[||] and Jean-Marie Lehn*[,†]

Contribution from the Laboratoire de Chimie Supramoléculaire, ISIS, Université Louis Pasteur, 8, allée Gaspard Monge, BP 70028, F-67083, Strasbourg, Cedex, France, Institut Européen des Membranes - IEM-CNRS 5635, Place Eugène Bataillon, CC 047, F-34095 Montpellier, France, European Synchrotron Radiation Facility, ESRF, BP 220, 38043, Grenoble Cedex, France, and Service Commun de RMN, 1, rue Blaise Pascal, F-67008 Strasbourg, France

Received March 26, 2003; E-mail: lehn@isis.u-strasbg.fr

Abstract: The binding of lead(II) cations to the terpyridine-type subunits of the helical ligand **1** leads to the self-assembly of different polynuclear metallosupramolecular architectures of nanometric size. Three different entities are generated and may be interconverted as a function of metal/ligand stoichiometry: a $[4 \times 4]$-Pb_{16}^{II} grid-type array **2**, a $[4 \# 4]Pb_{12}^{II}$ double-cross species **4**, and an intermediate complex **3**. The structures of **2** and **4** have been confirmed by X-ray crystallography; that of **3** is based on NMR spectral data. The interconversion of the three species generates dynamic diversity and represents an expression of constitutional dynamic chemistry. In the course of ion binding, the helical molecules of ligand **1** unwrap to yield fully extended strands arranged in perpendicular fashion in the architectures **2**−**4** generated. This process amounts to molecular motions in two directions which confer to the present systems characteristics of two-dimensional nanomechanical devices, capable of performing 2D-contraction/extension motions. The triple features of self-organization, dynamic interconversion, and potential addressability displayed by the processes described trace a self-fabrication approach to nanoscience and nanotechnology.

The spontaneous but controlled generation of functional supramolecular architectures by self-assembly has emerged as a major development of supramolecular chemistry toward the design of self-organizing systems of increasing complexity. In particular, the self-assembly of inorganic supramolecular entities is based on the implementation of ligands containing specific molecular information stored in the arrangement of suitable binding sites and of metal ions reading out the structural information through the algorithm defined by their coordination geometry.[1,2] Of special interest among the great variety of possible superstructures are those in which metals ions are arranged in a grid-type fashion, which present intriguing features as multisite species of interest for nanotechnology as eventual components of information storage devices.[3] Square $[2 \times 2]M_4^{II}$ grid-type assemblies (M = transition metal) based on tridentate binding subunits and octahedral[4] coordination have been actively studied in our laboratory, revealing a range of interesting structural[4a] and physicochemical (electrochemical,[4b] magnetic[4c]) properties. In view of both basic interest and potential applications, further extension to the self-assembly of higher order grids has been investigated. Thus, grids based on tetrahedral coordination containing arrays of 9 and 20 Ag(I) ions, $[3 \times 3]Ag_9^{I}$ [5a] and $[4 \times 5]Ag_{20}^{I}$,[5a] were obtained, as well as $[2 \times 3]$ and $[3 \times 3]$ grids containing six and nine octahedral coordination sites.[6] An extended square grid $[4 \times 4]Pb_{16}^{II}$ [7] based on an octahedral bisterpyridine coordination motif was obtained, where Pb^{II} ions

[†] Université Louis Pasteur.
[‡] Institut Européen des Membranes.
[§] European Synchrotron Radiation Facility.
[||] Service Commun de RMN.

(1) Lehn, J.-M. *Supramolecular Chemistry-Concepts and Perspectives*; VCH: Weinheim, 1995; Chapter 9.
(2) For a selection of recent reviews on metal ion mediated self-assembly, see, for example: (a) Baxter, P. N. W. In *Comprehensive Supramolecular Chemistry*; Atwood, J. L., Davies, J. E. D., MacNicol, D. D., Vögtle, F., Lehn, J.-M., Eds.; Pergamon: Oxford, 1996; Chapter 5, Vol. 9, pp 165−211. Constable, E. C. In *Comprehensive Supramolecular Chemistry*; Atwood, J. L., Davies, J. E. D., MacNicol, D. D., Vögtle, F., Lehn, J.-M., Eds.; Pergamon: Oxford, 1996; Chapter 6, Vol. 9, pp 213−252. Fujita, M. In *Comprehensive Supramolecular Chemistry*; Atwood, J. L., Davies, J. E. D., MacNicol, D. D., Vögtle, F., Lehn, J.-M., Eds.; Pergamon: Oxford, 1996; Chapter 7, Vol. 9, pp 253−282. (b) Saalfrank, R. F.; Bernt, I. *Curr. Opin. Solid State Mater. Sci.* **1998**, *3*, 407−413. (c) Olenyuk, B.; Fechtenkotter, A.; Stang, P. J. *J. Chem. Soc., Dalton Trans.* **1998**, *11*, 1707−1728. (d) Fujita, M. *Acc. Chem. Res.* **1999**, *32*, 53−61. (e) Caulder, D. L.; Raymond, K. N. *J. Chem. Soc., Dalton Trans.* **1999**, *8*, 1185. (f) Piquet, C. *J. Inclusion Phenom. Macrocyclic Chem.* **1999**, *4*, 361−391. (g) Saalfrank, R. W.; Demleitner, B. In *Transition Metals in Supramolecular Chemistry*; Sauvage, J. P., Ed.; John Wiley and Sons: New York, 1999; Chapter 1, pp 1−51. (h) Leininger, S.; Olenyuk, B.; Stang, P. J. *Chem. Rev.* **2000**, *100*, 853−908. (i) Swiegers, G. F.; Malefetse, T. J. *Chem. Rev.* **2000**, *100*, 3483−3537. (j) Swiegers, G. F.; Malefetse, T. J. *J. Inclusion Phenom. Macrocyclic Chem.* **2001**, *40*, 253−264. (k) Holliday, B. J.; Mirkin, C. A. *Angew. Chem., Int. Ed.* **2001**, *40*, 2022−2043. (l) Albrecht, M. *Chem. Rev.* **2001**, *101*, 3457−3497. (m) Seidel, S. R.; Stang, P. J. *Acc. Chem. Res.* **2002**, *35*, 972−983.
(3) For a comment, see ref 1, pp 199−201.
(4) (a) Hanan, G. S.; Volkmer, D.; Schubert, U. S.; Lehn, J.-M.; Baum, G.; Fenske, D. *Angew. Chem., Int. Ed. Engl.* **1997**, *36*, 1842−1844. (b) Ruben, M.; Breuning, E.; Gisselbrecht, J.-P.; Lehn, J.-M. *Angew. Chem., Int. Ed.* **2000**, *39*, 4139−4142. (c) Breuning, E.; Ruben, M.; Lehn, J.-M.; Renz, F.; Garcia, Y.; Ksenofontov, V.; Gütlich, P.; Wengelius, E.; Rissanen, K. *Angew. Chem., Int. Ed.* **2000**, *39*, 2504−2507.
(5) (a) Baxter, P. N. W.; Lehn, J.-M.; Fischer, J.; Youinou, M.-T *Angew. Chem., Int. Ed. Engl.* **1994**, *33*, 2284−2287. (b) Baxter, P. N. W.; Lehn, J.-M.; Baum, G.; Fenske, D. *Chem.-Eur. J.* **2000**, *6*, 4510−4517.
(6) Breuning, E.; Hanan, G. S.; Romero-Salguero, F. J.; Garcia, A. M.; Baxter, P. N. W.; Lehn, J.-M.; Wegelius, E.; Rissanen, K.; Nierengarten, H.; van Dorsselaer, A. *Chem.-Eur. J.* **2002**, *8*, 3458−3466.

Scheme 1. Structure of Ligands **1**, **5**, and **6**

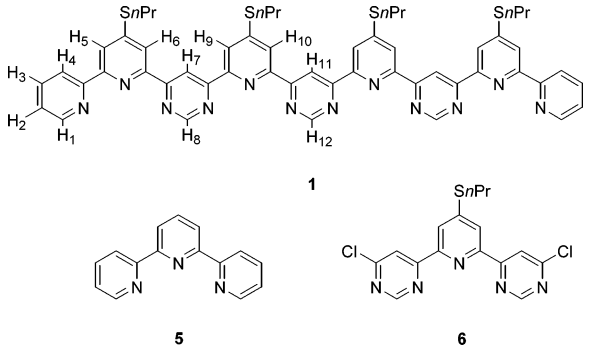

were selected as assembly sites because these large ions were expected to cause less ligand curvature than the small transition metal ions, which induce significant pinching of the coordination subunits.[8] The formation structure and stability of such large coordination networks gives access to a variety of supramolecular architectures, incorporating different arrays of metal ions, of precisely defined position and nuclearity, which may be expected to exhibit a wide variety of physicochemical properties.

Furthermore, a given ligand may generate different inorganic architectures depending on internal parameters (such as the nature of the binding subunit, the coordination geometry of the metal ion used, the ion/ligand stoichiometry) or on external factors (such as the nature of the medium, the presence of specific molecules or anions, etc). Thus, coordination equilibria allow the generation of dynamic libraries of metal complexes presenting features such as self-selection (as in helicate formation[9]), solid-state selection of a constituent of an equilibrating collection of complexes,[10] and reversible switching between different coordination arrays (as in the formation of different arrays of silver(I) ions in the course of the assembly of [3 × 3][11] and [4 × 5] grids).[12] The adaptive generation of a chloride ion receptor in the reversible interconversion of circular helicates[13] gave entry into dynamic combinatorial chemistry.[14]

Adaptive self-assembly was also found to occur in the medium-controlled reversible switching between a square and a hexagonal metallocyclophane architecture.[15] In view of the lability of the coordination bond, these and numerous recently described coordination processes[16] fall into the realm of dynamic chemistry[17] and may present a number of novel features such as cooperativity,[11a] diversity, selection, and adaptation.

(7) Garcia, A. M.; Romero-Salguero, F. J.; Bassani, D. M.; Lehn, J.-M.; Baum, G.; Fenske, D. *Chem.-Eur. J.* **1999**, *6*, 1803−1808.
(8) Hannan, G. S.; Arana, C. R.; Lehn, J.-M.; Baum, G.; Fenske, D. *Chem.-Eur. J.* **1996**, *2*, 1292−1302.
(9) Krämer, R.; Lehn, J.-M.; Marquis-Rigault, A. *Proc. Natl. Acad. Sci. U.S.A.* **1993**, *90*, 5394−5398.
(10) Baxter, P. N. W.; Lehn, J.-M.; Rissanen, K. *Chem. Commun.* **1997**, 1323−1324.
(11) (a) Marquis, A.; Kintzinger, J.-P.; Graff, R.; Baxter, P. N. W.; Lehn, J.-M. *Angew. Chem., Int. Ed.* **2002**, *41*, 2760−2764. (b) Hiraoka, S.; Yi, T.; Shiro, M.; Shionoya, M. *J. Am. Chem. Soc.* **2002**, *124*, 14510−14511.
(12) Baxter, P. N. W.; Lehn, J.-M.; Baum, G.; Fenske, D. *Chem.-Eur. J.* **2000**, *6*, 4510−4517.
(13) (a) Hasenknopf, B.; Lehn, J.-M.; Kneisel, B.; Fenske, D. *Angew. Chem., Int. Ed. Engl.* **1996**, *35*, 1838−1841. (b) Hassenknopf, B.; Lehn, J.-M.; Boumediene, N.; Dupont-Gervais, A.; Van Dorsselaer, A.; Kneisel, B.; Fenske, D. *J. Am. Chem. Soc.* **1997**, *119*, 10956−10962.
(14) Lehn, J.-M. *Chem.-Eur. J.* **1999**, *5*, 2455−2463.
(15) Baxter, P. N. W.; Khoury, R. G.; Lehn, J.-M.; Baum, G.; Fenske, D. *Chem.-Eur. J.* **2000**, *6*, 4140−4148.
(16) Seidel, S. R.; Stang, P J. *Acc. Chem. Res.* **2002**, *35*, 972−983.

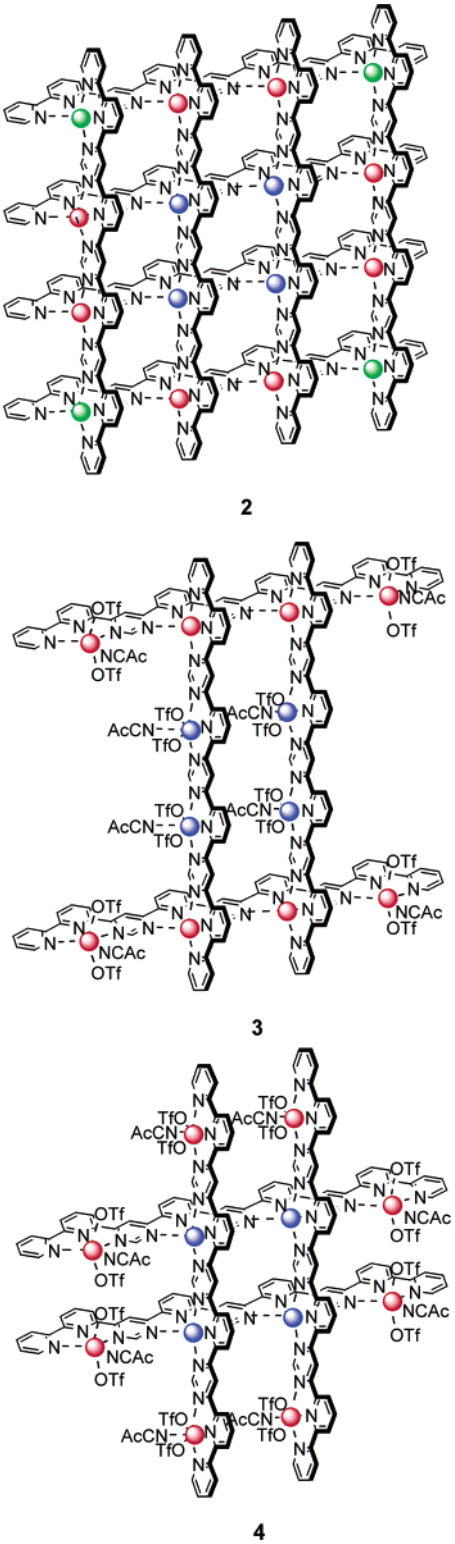

We describe here a study of the equilibrium binding of lead(II) ions to the tetratopic ligand **1** (Scheme 1),[7] leading to the identification of **2**−**4** of the possible coordination entities that may form.

The self-assembly of the [4 × 4]Pb_{16}^{II} grid-type complex **2** from ligand **1** and Pb^{II} ions was reported earlier.[7] We now describe the crystal structures of two complexes **3** and **4** and the nature of the species which are progressively and reversibly generated as increasing amounts of Pb(II) metal ions are added to a solution of ligand **1**.

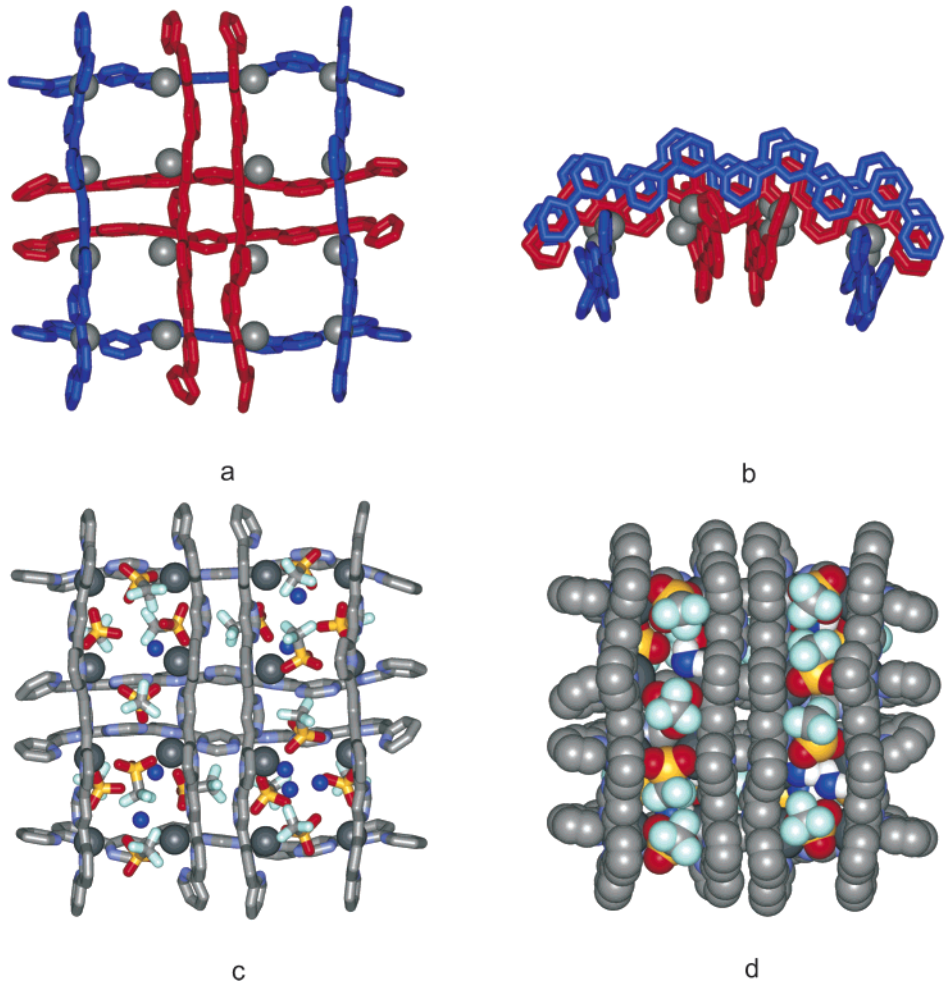

Figure 1. Crystal structure of the [4 × 4] grid complex **2**: $\mathbf{1}_8Pb_{16}^{II}$ (a) top view, (b) side view in stick representation; and $\mathbf{1}_8Pb_{16}^{II}Tf_{16}\cdot 8H_2O$ (c) stick representation, (d) space-filling representation. The lead(II) ions are shown as gray spheres.

Result and Discussion

Solid-State Structure of Multinuclear Pb^{II} Complexes of Ligand 1. [4 × 4]Pb_{16}^{II} Grid-type Architecture 2. It was shown earlier that a solution of ligand **1** and lead triflate in acetonitrile in 1/2 stoichiometry contained only a single entity identified as the grid-type complex **2** by ^1H and ^{207}Pb NMR spectroscopy. Layering such a 1/2 **1**/$Pb(CF_3SO_3)_2$ solution in acetonitrile with benzene/*i*-isopropyl ether (5/1, v/v) resulted in the formation of pale-yellow crystals which were investigated by X-ray crystallography. Only very poor crystals could be obtained, and tractable data could only be collected using a high-intensity synchroton X-ray source. Structure solution and refinement required accumulation of data from several crystals and very extensive treatment. After much effort, a crystal structure could be obtained which showed the complex to possess indeed a [4 × 4] grid-type structure and to be composed of 8 molecules of ligand **1**, 16 lead cations, 16 triflate counterions, and 8 water molecules $\mathbf{1}_8Pb_{16}^{II}Tf_{16}\cdot 8H_2O$ (Tf = $CF_3SO_3^-$) (Figure 1); 16 other triflate counterions and 1 molecule of water are located in close proximity. All ligands are fully coordinated through all of their nitrogen sites; they are warped, displaying a distorted octahedral coordination of the lead(II) ions and are in a cisoid conformation around all interheterocyclic C−C bonds. The average Pb−N distances are 2.57 Å (pyridine−N) and 2.70 Å (pyrimidine−N); they are similar to those found in the $[2 \times 2]Pb_4^{II}$ grid structure described earlier.[7]

The eight ligands **1** in **2** are arranged into two perpendicularly disposed sets of four outer and four inner ligands **1**, resulting in a set of four [2 × 2] subgrids rather than a regular [4 × 4] grid (Figure 1a,b).

The four inner ligands allow considerable overlap between the aromatic groups situated in a face-to-face stacking arrangement, with an average $\pi-\pi$ stacking centroid−centroid distance[18] of 3.62 Å corresponding to van der Waals contact. The Pb^{II} ions form a saddle arrangement with an average Pb−Pb distance of 6.3 Å and average inner angles of 89.5°. The coordination polyhedron around the lead ions reveals a hemi-directed structure,[19] and all Pb^{II} ions present a distorted seven-, eight-, or nine-coordinate geometry. The open faces of the metal ions are oriented toward the interior of the four $[2 \times 2]Pb_4^{II}$ grid subsets and are occupied each by one or two of the 16 internally coordinated triflate counterions (average Pb−O

(17) (a) Lehn, J.-M. In *Supramolecular Science: Where It Is and Where It Is Going*; Ungaro, R., Dalcanale, E., Eds.; Kluwer Academic Publishers: Norwell, MA, 1999; pp 287−304. (b) Lehn, J.-M. *Proc. Natl. Acad. Sci. U.S.A.* **2002**, *99*, 4763−4768.

(18) Janiak, C. *J. Chem. Soc., Dalton Trans.* **2000**, 3885−3896.

(19) Shimoni-Livny, L.; Glusker, J. P.; Bock, C. W. *Inorg. Chem.* **1998**, *37*, 1853−1867.

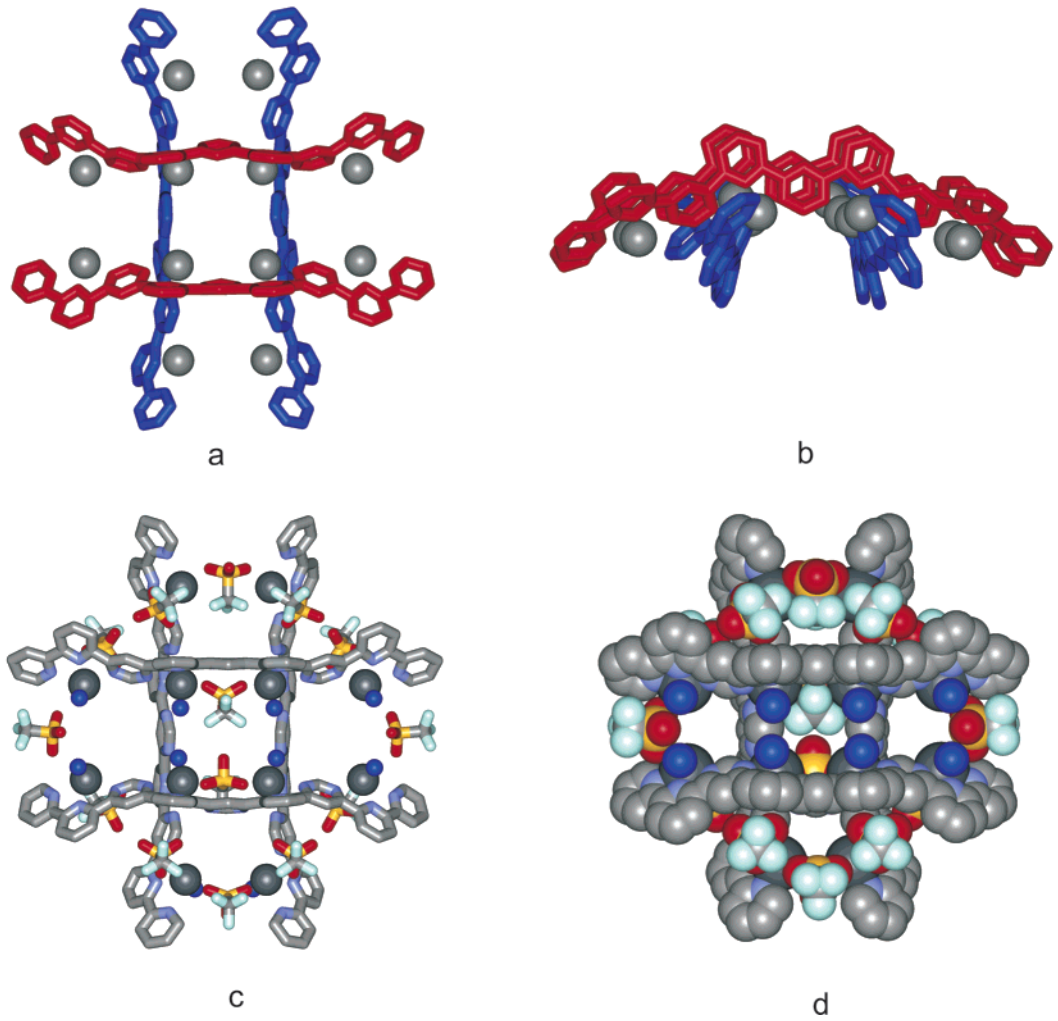

Figure 2. Crystal structure of the double-cross complex **4**: $\mathbf{1}_4Pb_{12}^{II}$ (a) top view, (b) side view in stick representation; and $\mathbf{1}_4Pb_{12}^{II}Tf_{12}\cdot 8H_2O$ (c) stick representation, (d) space-filling representation. The lead(II) ions are shown as gray spheres.

distance ~2.75 Å). The internal triflate counterions located as coordinating bridges between two adjacent lead atoms and the internally bound water molecules (average Pb−OH_2 distance ~2.64 Å) fill the interstices between the cations, so that all available void space between the inner and the outer ligands is filled (Figure 1c,d). Each square of four Pb^{II} ions is linked on three sides by bridging triflate counterions, with additional coordination sites filled by nonbridging triflate counterions or water molecules. The average centroid−centroid distance between inner and the outer ligands is 7.44 Å. In the crystal lattice, the complex cations pack into parallel layers which are alternately stratified above each other in a ABAB arrangement such that the outer edges of the squares of each layer are in van der Waals contact. These layers are connected by additional interaction between the S^{n}Pr moieties of each alternate layer. External triflate anions, water, and *i*-isopropyl ether solvent molecules fill the interstices between the cations so that all available space is filled.

[4 # 4]Pb_{12}^{II} Double-Cross-type Architecture 4. Layering a solution of a 1:4 molar ratio of **1**/$Pb(CF_3SO_3)_2$ in acetonitrile with benzene/*i*-isopropyl ether (5/1, v/v) resulted in the development of pale-yellow crystals which were investigated by X-ray crystallography. It revealed that this compound is a complex having a $\mathbf{1}_4Pb_{12}^{II}\cdot Tf_{12}\cdot 10H_2O$ [4 # 4] double-cross-type structure and is composed of 4 ligands **1**, 12 lead cations, 12 triflate counterions, and 10 water molecules (Figure 2). An additional 11 triflate counterions, 2 isopropyl ether, and 5 water molecules are situated in close proximity to the cationic complex; due to the poor quality of the crystals, one triflate counterion for charge neutrality could not be located. All ligands are warped and in a cisoid conformation around all interheterocyclic C−C bonds. The average Pb−N distances are 2.50 Å (pyridine N) and 2.60 Å (pyrimidine N); they are similar to those in the [4 × 4]Pb_{16}^{II} grid-type structure. The four ligands of **4** are arranged into two perpendicular sets (Figure 2a,b). The Pb^{II} ions are disposed along a planar double-cross with an average Pb−Pb distance of 6.75 Å and average inner angles of 90.1 Å. The 12 hemidirected lead ions of **4** are arranged into two sets, consisting of four fully coordinated interior ions and eight exterior ones coordinating each one terpyridine unit (Figure 2c,d). The open faces of the four interior leads ions are oriented into the interior of the internal [2 × 2]Pb_4^{II} grid, defined by the double-cross geometry, and are occupied by two coordinated triflate counterions located as coordinating bridges between two adjacent lead atoms (average Pb−O distance ~2.65 Å) with one water molecule bound to each lead ion (average Pb−OH_2 distance is ~2.65 Å). The eight terpy-coordinated exterior lead ions are coordinated to the eight external terpy-type sites of the four ligands

and bind 12 triflate counterions located either two-by-two as coordinating bridges between each two adjacent lead ions (average Pb−O distance is ∼2.7 Å) or singularly coordinated to the exterior. Water molecules are also bonded to some lead ions (average Pb−OH_2 distance is ∼2.49 Å).

In the crystal lattice, the cations pack into parallel layers which are alternately stratified above each other in a ABAB arrangement. The outer pyridines edges of each cross-grid are stacked two-by-two with an average $\pi-\pi$ stacking centroid−centroid distance of 3.70 Å corresponding to the van der Waals contact. These layers are connected by an additional interaction between the S^{n}Pr moieties of each alternate layer.

The X-ray crystallographic results allow the following conclusions to be made:

(1) The [4 × 4]Pb_{16}^{II} grid **2** and [4 # 4]Pb_{12}^{II} double-cross **4** architectures represent attractive arrays of lead ions, sets of ions dots[3,5] of well-defined arrangement and accessible in a single operational step by correct self-assembly of, respectively, 24 and 16 components through the formation of 96 and 48 coordinative bonds between the ligands and the lead(II) ions.

(2) The [4 × 4]Pb_{16}^{II} grid architecture **2** results from the appropriate design of the ligand which undergoes efficient self-assembly under the principle of "maximum coordination site occupation".[1,9] The hexadecanuclear coordination array is further stabilized by strong $\pi-\pi$ interactions between the inner ligands resulting in a robust double-cross core substructure composed of two pairs of nine $\pi-\pi$ stacking subsets. Additional stabilization is brought synergetically by internal bridge-type coordination of the lead cations by the triflate counterions which also decrease the total charge of the complex cation and the Coulombic repulsion between the Pb^{II} cations.

(3) The [4 # 4]Pb_{12}^{II} double-cross architecture **4** represents the best compromise, maximizing the number of Pb−N, Pb−CF_3SO_3, and Pb−OH_2 interactions so that all available void space between the ligands is filled. The average centroid−centroid distance between the ligands is now about 9.74 Å, the central square having dimensions similar to those of the [2 × 2] subgrids in **2**.

(4) The overall external dimensions of the [4 × 4]Pb_{16}^{II} **2** grid and of the [4 # 4]Pb_{12}^{II} double-cross **4** are 29 Å (ligand length) and 10.2 Å (height) (considering exact CC distances and omitting the S^{n}Pr grafted groups), while the total volumes are $V \approx 8.6$ nm^3 for **2** and 6.9 nm^3 for **4**. These geometric features place these entities within the nanostructural domain.

Controlled Generation and Interconversion of the Pb^{II} Arrays Formed by Ligand 1. The ability of a ligand such as **1** to form different metal complexes gives access to a diverse set of arrays of metal ions. The ability to control the generation and the interconversion of these entities provides, in principle, means for taking full advantage of the dynamic constitutional/combinatorial diversity that they offer. Such was the case in the interconversion of arrays of silver(I) ions in the course of the formation of a [3 × 3] grid[11] and in the equilibrium between a [4 × 5] grid with a quadrupole helix[12] as well as in the medium-induced adaptive exchange between a square and a hexagonal arrangement of copper(II) ions.[15] Furthermore, to control the generation of such supramolecular architectures, it is necessary to develop methods for their self-assembly as well as to determine the domains of stability of the corresponding extended arrays of nanometric dimension presenting a high metal nuclearity. As a step toward this goal, we decided to investigate the formation, the domain of existence, and the interconversion of the polynuclear complexes that may result from the binding Pb^{II} of cations to ligand **1** in various stoichiometric ratios. Such systems might form by self-assembly under mild conditions and be readily amenable to solution studies by ^{1}H and ^{207}Pb NMR.

Initial complexation studies revealed that addition of Pb$(CF_3SO_3)_2$ to an acetonitrile suspension of **1** caused a rapid dissolution of the ligand over a **1**/Pb^{II} molar ratio from 1:1 to 1:5.5. ^{1}H and ^{207}Pb NMR spectroscopy was used to follow the titration of a 0.02 mol dm^{-3} solution of **2** by a solution of Pb$(CF_3SO_3)_2$ in [D_3]acetonitrile to obtain information about the coordination behavior of **1** toward Pb^{II} ions.[20] Below a **1**/Pb^{II} molar ratio of 1:1.5, a very complex and broad spectrum was obtained, indicative of the presence of several exchanging species in solution. At a 1/1.5 **1**/Pb^{II} ratio, a dramatic simplification of the ^{1}H NMR spectrum was observed, yielding a series of peaks in approximately a 1:1 ratio, consistent with the presence of the [4 × 4]Pb_{16}^{II} grid-type complex **2** (75%) in slow exchange with other species presenting exchange-broadened signals. Further addition of salt led to the progressive conversion of these compounds into the final [4 × 4]Pb_{16}^{II} grid-type complex **2**, which was the only species present at the required **1**/Pb^{II} ratio of 1:2 (Figure 3b). The spectrum of the [4 × 4]-Pb_{16}^{II} grid **2** contained signals for ligand **1** located in two different magnetic environments in a 1/1 ratio, consistent with the presence of four outer and four inner ligands in the complex (Figures 3, 4).

The COSY and the ROESY spectra further reinforced this assignment as previously reported.[7] The ^{207}Pb NMR spectrum of **2** (Figures 3, 4) showed three signals in a 1:2:1 ratio, corresponding to lead cations in three different chemical environments.[7] The 2D ^{1}H−^{207}Pb NMR correlation spectra provided decisive information and confirmed the previous assignments of the Pb^{II} ions, giving a precise localization of the ions corresponding to the different lead signals: four in the corners, four in the interior, and eight at positions 2 and 3 on the edges (Figure 4).

When the **1**/Pb^{II} ratio was increased from 1/2 to 1/3, a more complex spectrum was obtained indicative of the presence of two slowly exchanging species in solution. The grid complex **2** was progressively converted into a new compound **3** (92% at a **1**/Pb^{II} ratio of 1/3). Further incremental increase in the **1**/Pb^{II} ratio caused a rapid nonlinear conversion of complex **3** into a new compound **4**: 55% of **4** at a **1**/Pb^{II} ratio 1/3.25 and exclusively **4** at a **1**/Pb^{II} ratio of 1/4, respectively (Figure 5). Species **3** and **4** were in slow exchange over the coexistence domain. The proton spectrum of **3** shows broadened signals that may be due to some kind of unidentified exchange process(es). Over a **1**/Pb^{II} ratio range from 1/4 to 1/5.5, only minor changes in chemical shift positions were observed and not a further apparent alteration in the species distribution (Figure 5).

Important support for the formulation of complexes **3** and **4** was afforded by analysis of the ^{1}H and ^{207}Pb NMR and of the 2D ^{1}H−^{207}Pb NMR correlation spectra. While the ^{1}H NMR spectrum of **3** was composed of two different sets of peaks indicating that ligand **1** was located in two different magnetic

(20) As the grid complex **2** forms and is stable in acetonitrile, but is destroyed in less coordinating solvents such as nitromethane, the titrations were performed in acetonitrile. The presence of small amounts of water does not significantly affect the formation of the complex.

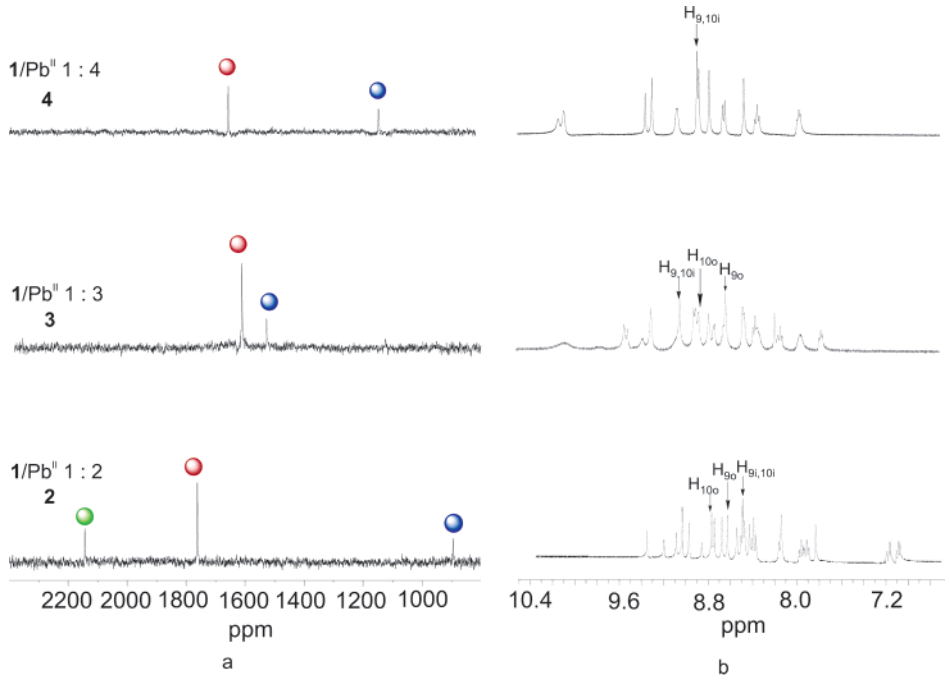

Figure 3. 83 MHz ^{207}Pb (a) and 500 MHz ^{1}H (b) NMR spectra of the complexes **2**, **3**, and **4** in CD_3CN at 0.02 M concentration; the ligand/Pb^{II} ions molar ratios are indicated on the left.

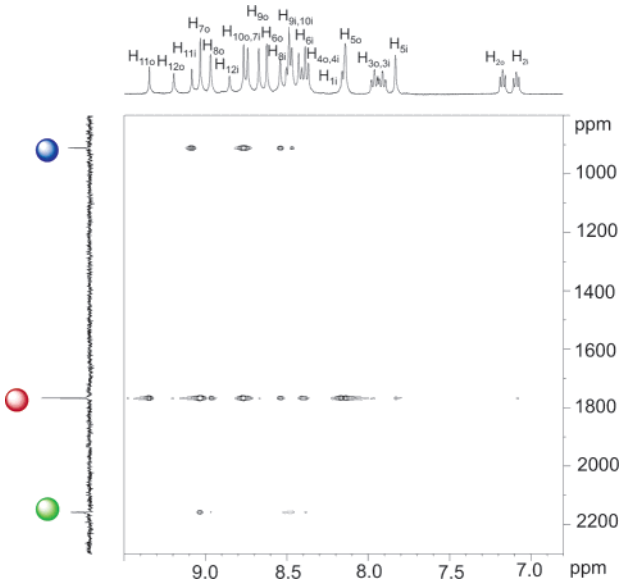

Figure 4. ^{1}H−^{207}Pb heteronuclear 2D-NMR correlation spectrum of the [4 × 4] grid complex **2** at 500 MHz (^{1}H) and 104 MHz (^{207}Pb); o, i: outer and inner ligands, respectively.

environments, that of **4** presented only one set of peaks for ligand **1** in a single magnetic environment (Figure 3b). On the other hand, the ^{207}Pb NMR spectra of both **3** and **4** (Figure 3a) showed two signals in a 1:2 ratio, corresponding to lead cations in two different chemical environments.

Crucial information about the nature of the species present was obtained from the 2D ^{1}H−^{207}Pb NMR correlation spectra of **3** and **4**:

For compound **3**, the ^{207}Pb^{II} signals may be assigned as follows. The peak of intensity 2 at $\delta = 1629$ ppm corresponds to lead ions coordinated at terminal pyridine moieties and results from the superposition of two lead signals [$Pb_{position}$ (number of vicinal Pb ions, type and number of coordination atoms)]: Pb_{vertex} (1, py_2, pym), Pb_{edge} (2, py_3, pym_3); the peak of intensity 1 at $\delta = 1578$ ppm corresponds to lead ions coordinated at central pyrimidine moieties: $Pb_{interior}$ (2, py, pym_2); the coordination environment of the lead(II) ions in the vertex and interior positions probably contains also two triflate anions and a molecule of acetonitrile, by analogy to that found in the crystal structure of complex **4**.

For compound **4**, the signals may be assigned as follows. The lead ions giving the peak of intensity 2 at $\delta = 1651$ ppm are coordinated at terminal pyridine moieties: $Pb_{terminal}$ (1, py_2, pym, $2TfO_2$, CH_3CN); the peak of intensity 1 at $\delta = 1138$ ppm corresponds to lead ions coordinated at central pyrimidine moieties: $Pb_{interior}$ (4, py_2, pym_4).

Additional support for the formulation of complexes **3** and **4** was afforded by examining the competitive complexation of Pb^{II} by the terpyridine **5** and the pympypym **6** ligands (Scheme 1). The ^{1}H NMR spectra of solutions of a 2:2:1 mixture of **5**/**6**/Pb^{II} showed an exclusive formation of the terpyridine $\mathbf{5}_2$Pb^{II} complex, which appears to be the most stable of the three possible complexes because it contains the highest number of the more basic py coordination sites. Further addition of 1 equiv of Pb^{II} gave a 1:1 mixture of the $\mathbf{5}_2$Pb^{II} and $\mathbf{6}_2$Pb^{II} complexes and no mixed ligand complex.

Furthermore, on addition of lead triflate to a diluted sample of **2** (0.004 M), direct conversion into **4** apparently occurred (Figure 5b). That **3** was not observed could be due to the presence of only a small amount together with exchange broadening, because such broadening is seen for some peaks in the proton spectrum of **3**. To reconcile the ^{1}H and ^{207}Pb NMR spectra of **3**, one might suggest that the central coordination sites are not fully occupied and that lead ions undergo exchange between these sites, causing a broadening of the pyrimidine proton signals without broadening of the lead signals.

The structural data above and the NMR spectroscopic results allow the following conclusions to be drawn:

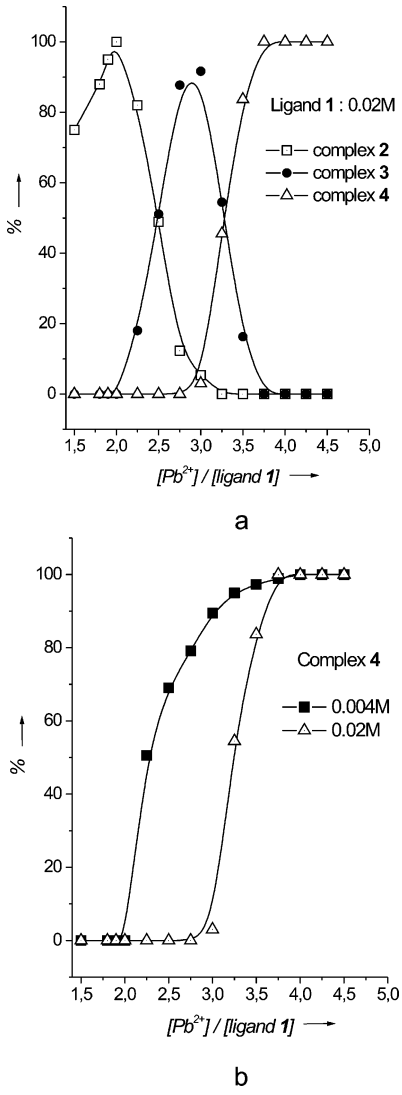

Figure 5. Distribution curves of the species formed on titration of a solution of ligand **1** in CD_3CN by a solution of lead triflate in CD_3CN at 25 °C (at an initial ligand **1** concentration of 0.02 M): (a) distribution of the complexes **2**, **3**, and **4**; (b) formation curves of complex **4** at two different initial concentrations of ligand **1**; the curves for **2** are omitted; no **3** was observable. The data points were obtained from the integration of characteristic proton NMR signals.

(1) The concentrated solution of **1**/Pb^{II} 1:3 contains complex **3**, composed of two outer and two inner ligands **1**, leading to a disymmetric rectangular geometry. On the other hand, at **1**/Pb^{II} > 1:3.25, it contains complex **4** composed of four ligands **1** disposed symmetrically like a double cross, in agreement with the crystal structure.

(2) No conversion into the streched out "sticklike" complex, similar to that generated from extended analogues of ligand **1**,[21] is observed, even at a **1**/Pb^{II} ratio as high as 1/5.5. This indicates that the [4 # 4] double-cross structure **4** is a very robust arrangement, stabilized by binding of triflate counterions into the central [2 × 2] grid substructure.

(3) In terms of inducing molecular shape changes resulting in molecular motion, the binding of Pb^{II} ions to the helical strand **1** causes its unwrapping to give fully extended strands incorporated in the [4 × 4] grid structure **2** or the [4 # 4] double-cross **4**. Whereas the conversion of helical strands into extended "stick" complexes reported earlier represents a one-dimensional molecular motion,[21] the formation of the grid **2** and double-cross **4** arrangements may be considered as generating two-dimensional molecular motion, the molecular helices leading to linear strands stretched out into two perpendicular directions (Scheme 2). One may surmise that it should be possible to induce sequential 2D-contraction/extension motions through pH modulation of reversible binding of the Pb^{II} ions in a manner similar to that described in previous work.[21]

Scheme 2. (a) One-Dimensional and (b) Two-Dimensional Molecular Motions Induced by Ion Binding to a Helical Ligand Strand, Generating Respectively a Stretched-Out "Sticklike" Entity[21]

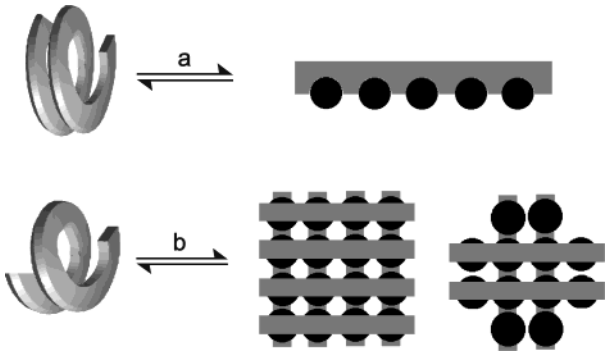

(4) The distribution curves of complexes **2**−**4** generated in the course of the titration of ligand **1** with lead triflate are shown in Figure 5. The [4 × 4] grid **2** is formed exclusively but requires correct stoichiometry. On the other hand, the [4 # 4] double-cross **4** is quite robust, remaining imperturbed on addition of metal ions beyond the required stoichiometry.

(5) In terms of programmed self-assembly,[1] the formation of the different metalloarchitectures **2**, **3**, and **4** underlines the fact that, despite the role of the strength of the coordination interactions and of maximal site occupation, other factors such as stacking, preferential pyridine coordination, and binding of anions (triflate ions stabilizing the highly charged network of lead cations) and of solvent molecules may interfere and influence the nature of the favored output species.

Conclusion

The above results describe the controlled formation and the interconversion of multiple metallosupramolecular architectures derived from the same ligand. Such dynamic diversity generation presents the features of constitutional dynamic chemistry.[17b] The formation of the complexes leads to the change in shape of the ligands from a helical strand to a fully extended form and involves molecular motions in two perpendicular directions, which confer to these systems the features of two-dimensional nanomechanical dynamic devices.[17,21−23]

The entities obtained are of nanometric size and display well-defined arrays of "ion dots"[3] generated by programmed self-assembly, which bear relation to arrays of nanofabricated quantum dots.[24] The three different ^{207}Pb NMR signals of the [4 × 4] grid **2** offer a means to address these ions by

(21) Barboiu, M.; Lehn, J.-M. *Proc. Natl. Acad. Sci. U.S.A.* **2002**, *99*, 5201−5206.
(22) Barboiu, M.; Vaughan, G.; Kyritsakas, N.; Lehn, J.-M. *Chem.-Eur. J.* **2003**, *9*, 763−769.
(23) (a) Lehn, J.-M. *Supramolecular Chemistry-Concepts and Perspectives*; VCH: Weinheim, 1995; Chapter 8. (b) Balzani, V.; Credi, A.; Raymo, F. M.; Stoddart, J. F. *Angew. Chem., Int. Ed.* **2000**, *39*, 3348−3391.
(24) Reed, M. A. *Sci. Am.* **1993**, *268*, 98.

Scheme 3. Reaction Sequence for the Preparation of Ligand **6**[a]

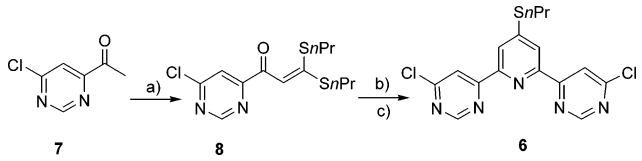

[a] (a) NaH, CS_2, ^{n}PrI, DMSO, room temperature; (b) ^{t}BuOK, THF; (c) AcOH/NH_4OAc, reflux.

electromagnetic radiation. If local changes at a given type of ionic site could be introduced, access to both information storage and retrieval might, in principle, be considered.[25]

The combined features of controlled generation and interconversion by self-organization, dynamic constitutional diversity, and potential addressability make processes and species such as those presented here of interest for the development of a supramolecular approach to nanoscience and nanotechnology through "self-fabrication", toward systems of increasing behavioral complexity.

Experimental Section

General Methods. All reagents were obtained from commercial suppliers and used without further purification. THF was distilled over benzophenone/Na. All organic solutions were routinely dried by using sodium sulfate (Na_2SO_4). Column chromatography was carried out on Merck alumina activity II-III. The ligand **1** was first isolated as a side product in the synthesis of more extended ligands,[26] and its direct synthesis was recently reported.[22] $Pb(OTf)_2$ was prepared from PbO and CF_3SO_3H as previously reported.[7] The microanalyses were carried out at Service de Microanalyses, Institut Charles Sadron, Strasbourg.

Compound 6: To a refluxing solution of **7** (50 mg, 0.32 mmol) and ^{t}BuOK (72 mg, 0.64 mmol) in dry THF (20 mL) was added a solution of **8** (100.1 mg, 0.32 mmol) (prepared from **7** according to ref 26) in dry THF (15 mL) under argon over a period of 2 h (Scheme 3). The solution was stirred overnight at room temperature, and acetic acid (1 mL) and NH_4OAc (1 g) were added to the reaction. The mixture was refluxed for 90 min, cooled, poured into water (100 mL), extracted with chloroform (3 × 100 mL), washed with saturated aqueous $NaHCO_3$ (100 mL), and dried with Na_2SO_4. After evaporation, the crude material was purified by flash chromatography (alumina/chloroform) to give **6** (85 mg, 85%). ^{1}H NMR ($CDCl_3$): δ = 9.09 (s, 2H), 8.64 (d, 2H J = 1.2 Hz), 8.53 (s, 2H), 3.24 (t, J = 7.9, 2H), 1.88 (sext, J = 7.9, 2H), 1.21 (t, J = 7.9, 3H). ^{13}C NMR ($CDCl_3$): δ = 13.85, 22.24, 33.24, 114.16, 119.74, 122.07, 158.32, 158.34, 162.44, 162.72, 162.81. Anal. Calcd for $C_{16}H_{13}N_5SCl_2$ (378.3 g/mol): C, 50.80; H, 3.46; N, 18.51. Found: C, 52.49; H, 3.36; N, 17.10.

NMR Spectroscopy. One-dimensional ^{207}Pb NMR spectra were recorded at 83 MHz on an Avance 400 MHz Bruker spectrometer at 25 °C. We used a 3 μs pulse enabling a correct spectral coverage, the spectral width being of 133 333 Hz. The repetition rate was in the range of 15 ms due to the fast relaxation rate on the lead nuclei (line width of 200−300 Hz). An average of 200 000 scans was generally sufficient to get good qualitative spectra. The data were processed after 40 Hz line broadening and a factor of 4 times zero-fill. The chemical shifts were referenced using $Pb(CF_3SO_3)_2$ versus $PbMe_4$ in [D_3]acetonitrile as the absolute lead chemical shift reference.

The ^{1}H NMR, COSY, and ROESY spectra were recorded on an Avance 500 MHz Bruker spectrometer, using a broad band inverse probe ϕ 5 mm, equipped with a z gradient coil. The chemical shift correlation was a magnitude detected mode COSY/GRASP with 2K data sets and 512 increments. The gradient intensities ratio was in the rate of 4/3/10. Processing data was done using a factor 3 sine bell shifted window function in both dimensions and a factor 4 zero-fill in the first dimension. The processing of data was done in the power mode.

The dipolar proton correlation was done using a ROESY-off[27] adiabatic experiment with 2K data and 512 increments. The relaxation rate was of 2 s. The spin lock was of 300 ms and 25 kHz adiabatic pulse at 3750 MHz off resonance, allowing a 54° spin lock. The processing of data was done using a factor 2 sine bell squared shifted window function with 2K real data in the acquisition dimension and a factor 4 zero-fill in the first dimension.

The heteronuclear shift correlation ^{1}H−^{207}Pb NMR was done at 104 MHz (^{207}Pb frequency) on a Avance 500 MHz Bruker spectrometer using an HMQC experiment with z gradient selection, the gradient intensity rates being 40/40/16.67. A total of 256 increments of 2K data points were acquired with 2 s interpulse delay and 8−40 transients per increment depending on the solution concentration. The spectral width in the first dimension of ~84 000 Hz is fairly compatible with an 11 μs 90° pulse, in the ^{207}Pb dimension, the HMQC experiment being not very sensitive to the 90° pulse intensity. Processing data was done using 2K real data with a factor 2 sine bell squared shifted window function in the second dimension and a factor 4 zero-fill and a factor 6−8 sine bell shifted window function in the first dimension.

X-ray Crystallographic Data for Complex 2 and Complex 4. X-ray diffraction data measurements for **2** and **4** were carried out at beamline ID11 at the European Synchrotron Facility (ESRF) at Grenoble. A wavelength of 0.32826 Å was selected using a double crystal Si (111) monochromator.

Single crystals of **2** ($C_{1856}H_{1584}N_{256}O_{420}F_{384}S_{384}Pb_{64}$) were grown from acetonitrile with benzene/*i*-isopropyl ether (5/1, V/V). Crystals were placed in oil, and a single yellow crystal of dimension 0.08 × 0.06 × 0.04 mm was selected, mounted on a glass fiber, and placed in a low-temperature N_2 stream. Data were collected using a Bruker "Smart" CDD camera system at fixed 2θ and reduced using the Bruker SAINT software.

The unit cell was monoclinic with space group of $P2_1/c$. Cell dimensions were a = 31.050(2) Å, b = 52.013(4) Å, c = 37.379(4) Å, β = 107.013(5)°, V = 57725(8) Å^3, and Z = 4. Of the 104 725 reflections collected from 1.57° ≤ θ ≤ 7.54°, 30 561 were unique with 18 083 having $I > 2\sigma(I)$. The lead atom locations were determined by Patterson methods using Shelxs.[28] Structure refinement was carried out with Shelxl.[29] Because of the poor quality of the crystal (rocking curves ~2°; no appreciable scattering beyond ~1.25 Å), it was necessary to place initially the ligands in theoretical positions with respect to the lead atoms. In further refinements, C−C and C−N bonds and angles were restrained such that the ligands were pseudosymmetric. Ligand positions, settings, and torsion angles were refined freely, and the triflate counterions and water molecules were located by subsequent Fourier recycling. Because of the poor data/parameter ratio, only the lead, sulfur, and triflate ions (as rigid bodies) were refined anisotropically. The final numbers of parameters and restraints were 4932 and 26 726, respectively. Hydrogen atoms were included at calculated positions by using a riding model. Final R factors were R_1 = 0.1248 (based on observed data), wR_2 = 0.3209 ($I > 4\sigma(I)$), and minimum and maximal residual electron densities were −1.8 and 1.9 e Å^{-3}.

Single crystals of **4** ($C_{984}H_{912}N_{192}O_{276}F_{216}S_{136}Pb_{48}$) were grown from acetonitrile with benzene/*i*-isopropyl ether (5/1, V/V). Crystals were placed in oil, and a pale yellow crystal of dimension 0.10 × 0.04 × 0.03 mm was selected, mounted on a glass fiber, and placed in a low-temperature N_2 stream. The unit cell was orthorhombic with a space group of *Pnma*. Cell dimensions: a = 29.582(4) Å, b = 38.279(6) Å, c = 36.713(5) Å, V = 41573(11) Å^3, and Z = 4. Reflections were

(25) For quantum-dot cellular automata, see, for instance: Lent, C. S.; Isaksen, B.; Lieberman, M. *J. Am. Chem. Soc.* **2003**, *125*, 1056−1063.
(26) Bassani, D. M.; Lehn, J.-M. *Bull. Soc. Chim. Fr.* **1997**, *134*, 897−906.
(27) Desvaux, H.; Berthault, P.; Birlirakis, N.; Goldeman, M. *C. R. Acad. Sci.* **1993**, *307 (II)*, 19−25.
(28) Sheldrick, G. M. *SHLXS97-A Program for Automatic Solution of Crystal Structures*; University of Göttingen, Germany, 1997.
(29) Sheldrick, G. M. *SHLXL97-A Program for Automatic Refinement of Crystal Structures*; University of Göttingen, Germany, 1997.

collected from $1.56° \leq \theta \leq 7.21°$ for a total of 35 552, of which 9309 were unique with 5286 having $I > 2\sigma(I)$. The best crystal of compound **4** which could be located was of even lower quality than that used for **2**, with average rocking curves greater than 3° and much of the data corrupted by split domains. The same methods described above were used to solve and refine the structure, although for compound **4** all of the triflate counterions could not be located. The final number of parameters was 1414 with 2262 restraints. Final R factors were $R_1 = 0.132$, w$R_2 = 0.3247$ ($I > 4\sigma(I)$), and minimum and maximal residual electron densities were -1.8 and 1.9 e Å^{-3}.

Acknowledgment. We thank Dr. A. M. Garcia for a first set of crystals of complex **2**. M.B. thanks the Collège de France for a postdoctoral fellowship.

Supporting Information Available: Crystallographic information (CIF). This material is available free of charge via the Internet at http://pubs.acs.org.

JA0301929